Studying the gelation mechanism of spherical colloidal systems with the bridging attraction using USANS

2022 Neutron School on Small Angle Neutron Scattering and Neutron Reflectometry

NIST Center for Neutron Research

USANS Experiment

John Barker, Peter Beaucage, Rachel Ford, Yun Liu

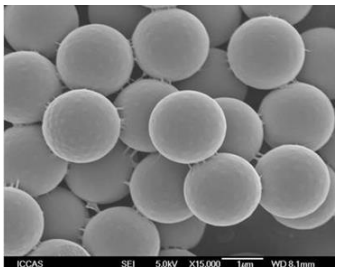

Abstract

The Ultra Small-Angle Neutron scattering (USANS) instrument at the NCNR is based on a Bonse-Hart design and can probe the structure with the length scale from about a few hundreds of nanometers to about twenty micrometers. It has been used to study a wide range of materials, such as shale, paints, and polymers. During this neutron school experiment, USANS is used to study the structures of colloidal suspensions to understand the physical mechanisms of the gel transition of this colloidal system. The studied system consists of large polystyrene (PS) particles and very small poly(N-isopropylacrylamide) (PNIPAM) microgel particles dispersed in aqueous solutions. There is no attraction among either large particles alone or small particles alone. However, when mixing the large and small particles together, there is a strong attraction between small and large particles. As a result, the small particle can serve as a bridge to attract neighboring large particles that introduce an effective attraction between large particles. This effective attraction between large particles is mediated by the properties of small particles and is termed as the bridging attraction. Using the USANS instrument, the particle size and the attraction strength can be experimentally determined by analyzing the scattering patterns. The extracted attraction strength allows us to position the studied samples in a theoretical phase diagram, from which the physical mechanisms of the gel transition can be revealed for this system. Various aspects of the experiment from the sample preparation and instrument setup to data treatment and interpretation will be investigated, and references are given for more in-depth study.

1. Introduction

In our everyday life, glass and gelation transitions are commonly observed phenomena in materials such as paint, shampoo, therapeutic drugs and metallic glass. When a material becomes a gel (or a glass), it changes from liquid to solid. Gel and glass materials usually have structures similar to their liquid states while their dynamics become significantly slower. The mechanisms of glass and gel transitions are still very poorly understood and considered as a grand challenge for many research fields.

Spherical colloidal particles in suspension are commonly used as model systems to investigate these transitions as we can control the effective interactions between colloidal particles. Sometimes, we can even visualize and track the trajectories of individual particles and observe details of structure and dynamics for a colloidal system during the transition. Glass transitions usually happen at high concentrations. For example, the glass transitions introduced by the pure excluded volume effect (hard sphere interaction) requires the volume fraction up to about 58% in order to change from a liquid state to a solid glassy state. Gelation transitions, however, usually happen at relatively low particle concentrations. This experiment focuses on understanding the gelation transition of a colloidal system.

In order to introduce a liquid-to-gel transition, particles need to have attractive interactions between them that drives the cluster formation. When the attraction strength and concentration are large enough, the size of clusters can become large enough to form percolated clusters. A percolated cluster is a cluster large enough to span through the whole system, i.e. the size of a percolated cluster is as large as the size of a sample. For a given interaction potential, the minimum concentration needed to generate at least one percolated cluster is defined as the percolation transition concentration. The percolation transition concentration is a function of the inter-particle potential and concentration. When the attraction is too strong, it can introduce the so-called gas-liquid (or liquid-liquid) phase separation, for which the suspension becomes two separated phases: one is rich with colloidal particles, and another is poor with colloidal particles. [1]

For colloidal systems with a short-range attraction, the equilibrium phase diagram that includes the percolation transition and gas-liquid phase transition have been determined already. (In colloidal systems, attractive interactions ranging less than about 15% of the diameter of particles are generally considered short-ranged attractions.) For any experimental systems, if we can determine the effective interparticle potential, the state of the studied samples can be then mapped into this equilibrium phase diagram.

Unlike the gas-liquid phase transition, the gelation transition is considered as a non-equilibrium state. Theoretically predicting the gelation transition has been difficult or nearly impossible. Experimentally, the gelation transition can be determined by studying the rheological behavior of samples. In a typical gel system, the storage modulus G’ is larger than the loss modulus G” while G’ is smaller than G” in liquid states. Hence, the gelation transition of a colloidal system can be determined by measuring G’ and G” using a rheometer.

The relative location of the gelation boundary in the equilibrium phase diagram for a short-range attraction system seems to be dependent on the type of systems. There had been some early studies claiming that the gelation transition in spherical colloidal systems is due to the frustrated liquid-liquid phase transition. And thus the gelation boundary of spherical systems with short-range attraction is close to the liquid-liquid phase boundary. Some other works believed that the gelation boundary should be close to the percolation transition instead of the liquid-liquid phase transition boundary. In fact, a system needs to have percolated clusters to form gel.

In this experiment, we try to determine the effective interaction potential between large colloidal particles in a colloidal system with so-called bridging attraction so that we can determine the boundary of the gelation transition in the equilibrium phase diagram.

2. Understanding USANS/SANS patterns from a colloidal system: form factor, structure factor and the interaction.

2.1. Our experimental system.

In this experiment, mixed suspensions of large hard PS microspheres (MS) and small soft PNIPAM microgels (MG) are used as model system to investigate the static properties of suspensions (see Figure 1):

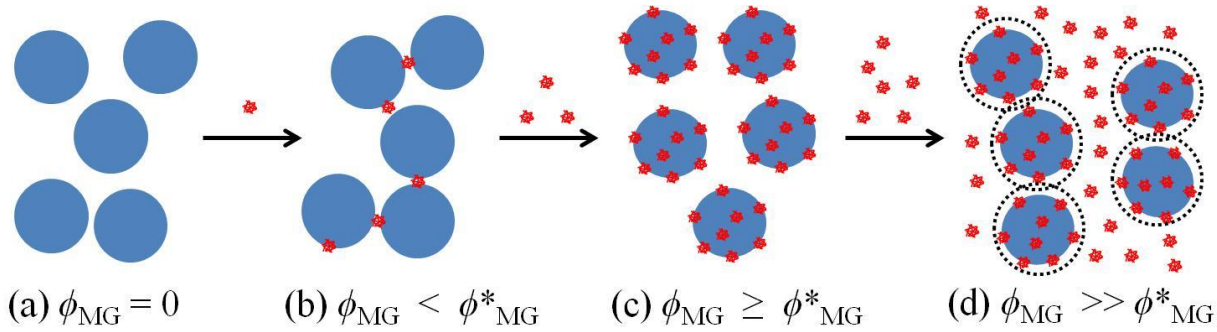

Figure 1: Schematic illustration of clustering (or gelation) of the large PS microspheres with increasing concentrations of small PNIPAM microgel (ϕ_{MG}) [2]. The microspheres, microgels and depletion layers are represented by solid blue circles, solid red circles, and dotted circles, respectively. a) bare MS stable in solution b) bridging between MS induced by MG c) above a critical MG concentration ϕ^*_{MG} the MS disperse freely again d) at high MG concentration there is evidence for MS clustering.

The small microgel particles can be reversibly adsorbed at the surface of large microspheres. The adsorbed small particles can attract neighboring large PS colloidal particles and serve as a bridge (See Figure 1 (b)). We are interested in studying the phase behavior of large colloidal particles only. Without the need to know the details of the behavior of small particles, the existence of small particles introduces an effective attraction between large colloidal particles. This type of attraction in our system is termed as *the bridging attraction*. Note that if small particles do not like the surface of large particles in a binary particle system,

the effective attraction generated by small particles are called the depletion attraction, which is different from the bridging attraction discussed here.

Typically, a short-range interaction potential between particles can be approximated by the following square well potential:

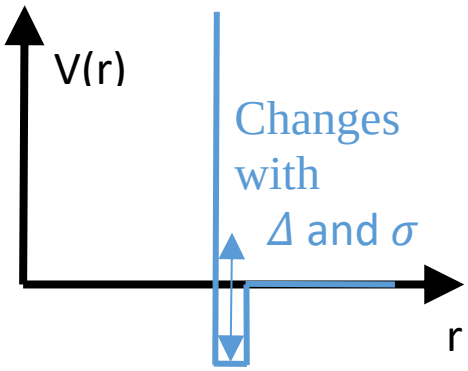

$$u(r) = \begin{cases} \infty & r < \sigma \\ -u_o & \sigma < r < \sigma + \Delta \\ 0 & r > \sigma + \Delta \end{cases}$$

Figure 2: Schematic of the Baxter's sticky hard sphere model, where σ is the diameter of the microsphere and Δ corresponds to the comparably thin layer of microgels surrounding it.

The strength of this short-ranged bridging attraction can be tuned by varying the small microgel concentration for a fixed volume fraction of large microspheres (ϕ_{MS}). As the concentration of microgels (ϕ_{MG}) is increased, the initially stable bare microspheres aggregate via bridging by the smaller particles, and disperse freely when adsorption of microgel on the surface of the microspheres reaches saturation.

It has been shown that for various systems with different attraction ranges and strengths, the potential parameters can be converted into two dimensionless parameters that control the phase diagram of colloidal systems with a short-ranged square-well potentials:

$$\tau = \frac{1}{12\varepsilon} e^{-\frac{u_0}{kT}}$$

$$\varepsilon = \frac{\Delta}{\sigma+\Delta} \qquad (1)$$

where u_0 is the attraction potential between two neighboring particles and kT represents the thermal energy. The square well potential can be approximated by the so-called sticky hard sphere system, whose function form was first proposed by R. Baxter in 1960s [3]:

$$V(r) = \lim_{\Delta \to 0} \begin{cases} \infty & r < \sigma \\ k_B T \ln\left[12\tau\left(\frac{\Delta}{\sigma+\Delta}\right)\right] & \sigma \le r \le \sigma + \Delta \\ 0 & r > \sigma + \Delta \end{cases} \qquad (2)$$

τ can be considered as an effective temperature; Large τ means a weak attraction (high temperature) and small τ values correspond to a strong attraction (low temperature).

The general equilibrium phase diagram for colloidal systems with a sticky hard sphere interaction can thus be shown in a $\tau - \phi$ plane as the following [3]:

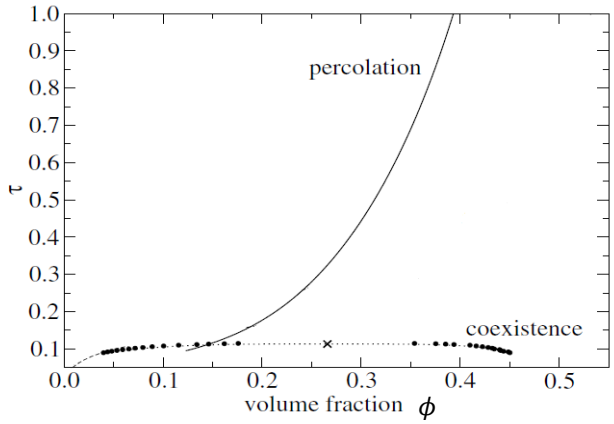

Figure 3: The general phase diagram expressed in volume fraction ϕ and effective temperature τ.

This generalized phase diagram can be also shown in a different way by replacing τ with the normalized second virial coefficient $B_2^* = B_2 / B_{2,HS}$, where B_2 is the second virial coefficient for the sticky hard sphere interaction and $B_{2,HS}$ is the second virial coefficient for a system with only hard sphere interaction. The relation between τ and B_2^* is

$$B_2^* = 1 - (4\tau)^{-1} \qquad (3)$$

(B_2^* or τ can be obtained by fitting the USANS data.) Note: The second virial coefficient B_2 is the first order correction of the equation of state for the deviation from the ideal gas law. In general, it can be expressed as: $B_2 = -2\pi \int (e^{-u(r)/k_B T} - 1) r^2 dr$, where $u(r)$ is the interaction potential between particles. For a hard sphere system, $B_{2,HS} = 4V$ with V the volume of the sphere. An equilibrium phase diagram for a sticky hard sphere system can be also plotted as in Fig. 4:

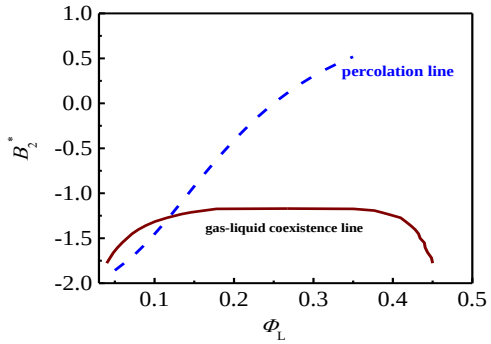

Figure 4: The general phase diagram in B_2^* and ϕ.

The figures 3 and 4 are equivalent to each other. Both are commonly used in the literature.

In a sticky hard sphere system, the gas-liquid transition is very flat (See Figure 4). It has been shown that, for some colloidal systems, the B_2^*-value close to the gelation transition is also very similar to its value at the gas-liquid coexistence line [4]. Hence, there has been a general feeling that the gelation transition of spherical colloidal particles is a frustrated gas-liquid phase separation. This may be a general feature of the gelation transition of spherical colloidal particles at low concentrations (and is true for our system as well).

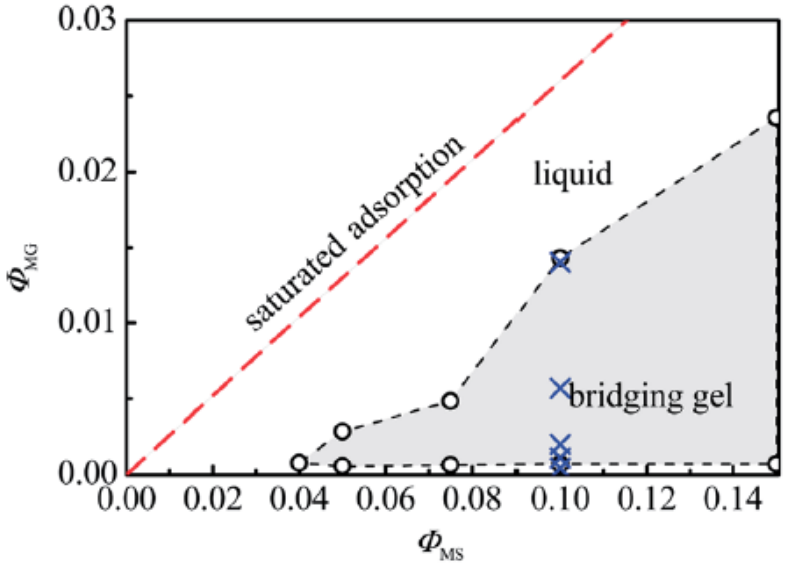

Figure 5: Phase diagram for the PS/PNIPAM-mixtures at low volume fractions: The open circles and dotted lines provide an estimated phase border established in previous measurements. The blue crosses represent the concentration used in our experiment.

In this experiment we use mixtures of Polystyrene and PNIPAM in water, the amount of PS will be kept constant at 10%$_{weight}$ and the PNIPAM concentration varies between 0-2%$_{weight}$ (see Figure 5). By fitting the USANS data from these samples, we can obtain the interaction potential information for various "positions" in the bridging gel state.

We know the equilibrium phase values for the percolation and the gas-liquid coexistence (see Figure 4). The question is: **How do these values compare to the values for the gelation transition in our system?**

To answer this question, we fit the measured scattering patterns to find the interaction potential, calculate the normalized second virial coefficient B_2^* for our data and insert these values into Figure 4 and check this way if the gelation transition in our system follows a similar physics mechanism.

2.2 How can a scattering experiment help determine interaction potential information?

In a liquid system at equilibrium conditions, the relative positions of colloidal particles are governed by the inter-particle potential. Any change of the potential affects the arrangement of colloidal particles in

solutions and will be reflected by a corresponding change in the scattering pattern. For a monodisperse hard-sphere system the coherent scattering pattern $I(q)$ can be expressed as

$$I(q) = AP(q)S(q) \quad (4)$$

where $A = \phi V \Delta\rho^2$, and ϕ, V, and $\Delta\rho$ are the volume fraction of the particles, the particle volume and the scattering length density contrast term respectively (see section 4.1); $P(q)$ is the normalized form factor, which is only related with the shape of a particle, and $S(q)$ is the inter-particle structure factor that is related with the inter-particle potential.

$S(q)$ is essentially a measure of the correlation function of the relative positions of the center of mass of particles. If a system is at equilibrium, S(q) can be determined by the inter-particle potential and calculated using statistical mechanical theories. The details of how to calculate S(q) is beyond the scope of this simple lecture (see [1] for details).

For a sample at liquid states, at relatively low concentrations, $S(q) \approx 1$. The scattering pattern of a dilute sample is thus determined by the form factor as $I(q) = AP(q)$. Once we have the information for $P(q)$ at small concentrations, we can extract $S(q)$ at higher concentrations.

2.3. Why use USANS?

Our experiment is designed to identify the interaction potential among the PS particles at different conditions close to the gelation boundaries due to the bridging attraction. As aforementioned, the gelation transition boundary has been previously determined with a rheometer. Because the size of the large microsphere is about 1μm, its length scale is within the range of the length scales probed by USANS. And from the USANS scattering curves, we can extract the attractive potential information for different microgel concentrations.

Generally, static light scattering can access similar length scales. The contrast in light scattering arises from the difference in the refractive index between the particle and water. At high concentrations, our samples have a white color. Hence, there will be too much multiple scattering so that the light scattering is not a correct tool for this. And, ultra-small angle x-ray scattering (USAXS) does not generally reach as low q as USANS. In addition, x-rays (particularly at synchrotron sources) can damage samples. USANS also overlaps in length scale with optical microscopy. However, since our samples are not transparent to light at large concentrations, it is difficult to study them with optical microscopes. SANS/USANS is therefore an ideal probe for the structure of these systems. The combination of SANS and USANS allows measurement of bulk samples over the whole relevant size range with no risk of sample damage.

3. The USANS Instrument

Fundamentally, a SANS/USANS experiment measures the number of neutrons scattered as a function of scattering angle. Since the size probed is inversely proportional to angle, to examine larger objects, we

need to measure scattering at smaller angles. In the case of a "pinhole" SANS instrument this is achieved by changing the distance of a two-dimensional detector from the sample. The smaller angle a detector element subtends, the further the detector is from the sample.

The SANS instruments at the NCNR can measure the q value down to $8x10^{-4}Å^{-1}$ at their maximum sample to detector distance using lenses to focus the neutron beam. This implies a maximum size of measurable objects of approximately 500 nm. One can imagine simply making longer and longer instruments to study larger and larger objects. However there are limitations to that approach. Firstly, neutrons have mass and thus are affected by gravity. They fall on a parabolic path as they travel from the source to a detector. Secondly, the collimation requirements for a longer instrument reduces the neutron flux onto the sample and increase the counting times. The count rate at the detector varies with the fourth power of the resolution. There is an alternative to a pinhole instrument using crystal diffraction before and after the sample in order to determine angular changes in the scattered beam. Such an instrument design is known as a Bonse-Hart type or Double-Crystal diffractometer (see Figure 6).

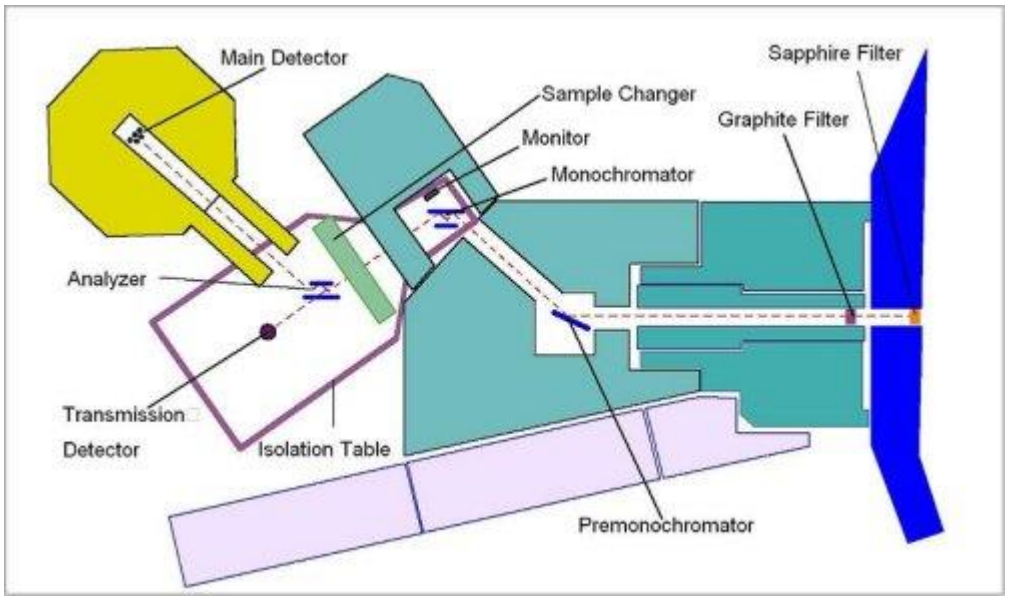

Figure 6: Schematic layout of the BT-5 USANS instrument. The dashed line indicates the beam path. The measured scattering angle, or momentum transfer q, is determined by rotation of the analyzer crystal.

Figure 6 shows the schematic layout of the NCNR USANS instrument which is located on beam tube 5 (BT-5). A channel cut silicon crystal (monochromator) directs the neutron beam onto the sample, where the neutrons are scattered. A second identical channel cut crystal (analyzer) is then placed in the scattered beam path and rotated to select the scattering angle to be analyzed and diffract the neutrons scattered at that angle into the detector. An experiment consists of rotating the analyzer to a series of angles and counting the number of neutrons that reach the detector. The intensity of scattering on the detector after background correction in a USANS experiment is given by

$$I_{cor}(q) = \varepsilon I_{beam} \Delta\Omega_A d_s T \left(\frac{d\sum_s(q)}{d\Omega}\right) \qquad (5)$$

where

ε is the detector efficiency

I_{beam} is the number of neutrons per second incident on the sample

d_s is the sample thickness

T is the sample transmission
$\Delta\Omega_A$ is the solid angle over which scattered neutrons are accepted by the analyzer
$\frac{d\sum_s(q)}{d\Omega}$ is the measured differential macroscopic scattering cross section, which is the true cross section modified by the instrumental resolution function.

The aim of a SANS/USANS experiment is to obtain the differential macroscopic scattering cross section $\frac{d\Sigma}{d\Omega}$ from I_{meas}. How we can go through that process is described later. But first we need to decide how to prepare our samples for the measurement.

4. Planning the Experiment

Given the stated objectives of the experiment and knowledge of the instrument, how do we prepare the experiment to maximize our chances of scientific success? Here we discuss some of the issues that are worth considering before an experiment.

4.1. Scattering Contrast

In order to have enough scattering intensity, there must be scattering contrast between, in this case, the spherical particles and the solvent. As shown previously, the absolute intensity of the neutron scattering can be expressed as $I(Q) = \phi V \Delta\rho^2 P(Q) S(Q)$. Hence, the scattering is proportional to the scattering contrast, $\Delta\rho^2$, where

$$\Delta\rho = \rho_1 - \rho_2 \qquad \leftarrow \text{Scattering Contrast} \qquad (6)$$

and ρ_1 and ρ_2 are the scattering length densities (SLD) of the microspheres and the solvent, respectively.

Recall that SLD is defined as $\rho = \frac{\sum_{i=1}^{n} b_i}{V}$ (7)

where V is the volume containing *n* atoms, and b_i is the (bound coherent) **scattering length** of the i^{th} atom in the volume V. V is usually the molecular or molar volume for a homogenous phase in the system of interest.

The SLD of each component can be calculated from the above formula, using a table of the scattering lengths of elements [4]. (The scattering length of different elements can be found at the NCNR website: https://www.ncnr.nist.gov/resources/n-lengths/ [5], or it can be calculated using the interactive *SLD Calculator* at the NCNR's Web pages (http://www.ncnr.nist.gov/resources/index.html). In SANS experiments it is a common practice to deuterate one or more components to increase the contrast for the component under study. In particular, deuterating the solvent removes much of the incoherent background from the hydrogen, which is a limiting factor for many samples for measurements at high q (above 0.2 $Å^{-1}$), but this is not relevant for the USANS experiment.

Material	Chemical Formula	Mass Density (g/cc)	SLD (cm^{-2})
Water	H_2O	1.0	-0.56×10^{10}
Heavy water	D_2O	1.1	6.33×10^{10}
Poly Styrene	$(C_8H_8)_n$	1.05	1.41×10^{10}
Poly(N-isopropylacrylamide)	$(C_6H_{11}NO)_n$	1.1	0.05×10^{10}

Table 1. The scattering length densities (SLD's) for the components used in this experiment. Note that these values are not precise, as the density of the material might differ from the literature values and especially for the PNIPAM gel the porous soft particles absorb water in solution.

In our samples, 50%-deuteration of the solvent is used to match the mass density (not the SLD!) of Polystyrene. This prevents sedimentation of the MS particles, the scattering contrast (neglecting the MG contribution) is $\Delta\rho = 1.48 \times 10^{10} cm^{-2}$. This value could be more than tripled using 100% D_2O as solvent and rotating the samples in the tumbler cell holder, but by matching the density the kinetic forces on the particles are reduced and historically the same samples have been examined in shear experiments as well. Also, by lowering the contrast multiple scattering is reduced (see section 4.3.).

There may be concerns that PNIPAM microgels may also contribute significantly to the scattering intensity. As it turns out, the PS particles are so large that they dominate the USANS signal.

4.2. Sample Thickness

H**ow thick should one sample be?** Recall that the scattered intensity is proportional to the product of the sample thickness, d_s and the sample transmission, T. It can be shown that the transmission, which is the ratio of the transmitted beam intensity to the incident beam intensity, is given by

$$T = e^{-\Sigma_t d_s}, \qquad (8)$$

where $\Sigma_t = \Sigma_c + \Sigma_i + \Sigma_a$, i.e. the sum of the coherent, incoherent and absorption macroscopic cross sections. The absorption cross section, Σ_a, can be accurately calculated from tabulated absorption cross sections of the elements (and isotopes) if the mass density and chemical compositions of the sample are known. The incoherent cross section, Σ_i, can be estimated from the cross section tables for the elements as well. The coherent cross section, Σ_c, can also only be estimated since it depends on the details of both the structure and the correlated motions of the atoms in the sample. This should be no surprise as Σ_c as a function of angle is the quantity we are aiming to measure! The scattered intensity is proportional to $d_s T$ and hence

$$I_{meas} \propto d_s e^{-\Sigma_t d_s} \qquad (9)$$

which has a maximum at $d_s = 1/\Sigma_t$ which implies an optimum transmission, $T_{opt} = 1/e \approx 0.37$. The sample thickness at which this occurs is known as the "1/e-length". The NCNR web based SLD calculator provides estimates of Σ_i and Σ_a and gives an estimate of the 1/e-length as well as calculating the SLD.

4.3. Multiple Scattering

The analysis of small angle scattering data assumes that a neutron is scattered only once when passing through a sample so that the scattering intensity is simply related to the structure of the sample. However, if the scattering of a sample is very strong, multiple scattering may contribute significantly to the scattering signal. The analysis of a signal with strong multiple scattering is very challenging [6] and, sometimes, is essentially impossible. Thus when Σ_c is significantly larger than $\Sigma_i + \Sigma_a$ the thickness should be chosen such that the transmission due to the coherent scattering remains larger than 0.9, rather than 0.37 to avoid problems with the multiple scattering effect.

In this experiment, the sample thickness has been set to 1 mm.

4.4. Required q range

The q range that is routinely accessible using the BT-5 USANS instrument is $5x10^{-5}$ Å^{-1} to $5x10^{-3}$ Å^{-1}. Both low q and high q limits are in practice determined by whether there is measurable scattering above background since the analyzer can be set to count at any value of q. The high q value chosen for an experiment is usually determined by the length scales of relevance to a sample and whether overlap with the SANS measurement regime is required. Figure 7 shows the accessible q ranges of the SANS and USANS instruments. In this experiment we will be measuring to approximately $2x10^{-3}$ Å^{-1}.

5. Collecting data

As discussed earlier, the experiment consists of scanning the analyzer through a series of angles and counting the scattered intensity on the detector. The first step before collecting the scattering data, therefore, is to decide which angles to measure at and how long to count at each.

5.1. Configuring the instrument

We need to measure over a range of angles spanning two orders of magnitude in q and an appropriate q-spacing at low q-values would lead to a huge excess of data points at around q = $1x10^{-3}$ Å^{-1}.

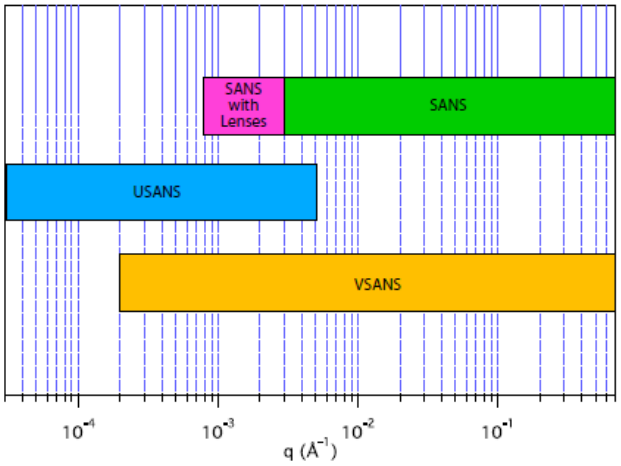

Figure 7: Comparison of the accessible q ranges of the BT-5 USANS instrument, NG-3 and NG-7 SANS instruments and the VSANS instrument currently under construction.

Thus we divide the data collection into six separate equally spaced scans, with each scan having roughly double the q spacing of the previous one. In the region, where the intensity varies greatly, we use closely spaced steps and increase the step size gradually as the intensity variation decreases. Furthermore, we count for short times where scattering intensity is high , and gradually increase the counting times as the intensity diminishes. The first scan spans the main beam and the peak intensity from that scan is used to determine the q = 0 angle, to scale the intensity into absolute units and to determine the sample transmission.

5.2. What measurements to make

To correct the instrument "background", a measurement of scattering without the sample is needed. Counts recorded on the detector can come from three sources: 1) neutrons scattered by the sample itself; 2) neutrons scattering from something other than the sample, but which pass through the sample; and 3) everything else, including neutrons that reach the detector without passing through the sample (stray neutrons or so-called room background) and electronic noise in the detector itself. In order to separate these contributions we need to make three separate measurements:

1. Scattering measured with the sample in place (which contains contributions from all three sources listed above), I_{sam}

2. Scattering measured with an empty sample holder in place (which contains contributions from sources 2 and 3 above), I_{emp}

3. Counts measured with a complete absorber at the sample position (which contains only the contribution from source 3 above), I_{bgd}

The I_{bgd} on the USANS instrument is predominantly due to fast neutrons. This background is independent of instrument configuration as the fast neutrons are not coming along the beam path. It has been measured and is 0.018 s^{-1}, which equals 0.62 counts per 10^6 monitor counts. Thus we do not usually measure a blocked beam run on USANS but use a fixed value for I_{bgd}.

5.3. How long to count

The uncertainty of the counting number due to the stochastic nature of the radiation (here, neutron) beam is important to understand the statistical error bar built into the scattering signal you collect. This uncertainty, or more precisely the standard deviation σ in the number of counts recorded in time, is given by $\sigma = \sqrt{N(t)}$. Here $N(t)$ is the total number of counts at certain detector position after counting for time t. Therefore, the relative error, $\sigma / N = 1/\sqrt{N} = 1/\sqrt{\gamma t}$, where γ is the average counting rate of a sample. Thus increasing the counting time by a factor of four will reduce the relative error, σ / N by a factor of two. If there are 1000 total counts per data point, the standard deviation is $\sqrt{1000}$, which is approximately 30, giving a relative uncertainty of about 3%, which is good enough for most purposes.

A related question is how long the empty cell measurements should be counted relative to the sample measurement. The same $\sigma = \sqrt{N(t)}$ relationship leads to the following approximate relationship for optimal counting times

$$\frac{t_{\mathrm{bgd}}}{t_{\mathrm{sam}}} = \sqrt{\frac{CountRate_{\mathrm{bgd}}}{CountRate_{\mathrm{sam}}}} \tag{10}$$

Hence if the scattering from the sample is weak, the background should be counted for as long as (but no longer than!) the sample scattering. If, however, the sample scattering count rate is, say, 4 times greater than the background rate, the background should be counted for only half as long as the sample. Since the scattering usually becomes much weaker at larger q, the time spent per data point increases with angle and the high q scans dominate the overall counting time.

5.4. Sample Transmission

The sample transmission is determined in two ways.

5.4.1. Wide angle transmission

A separate transmission detector (see figure 6), located behind the analyzer, collects all neutrons not meeting the Bragg condition for the analyzer. When the analyzer is rotated to a sufficiently wide angle from the main beam orientation this transmission detector counts both the direct beam intensity and the coherently small angle scattered intensity. Thus the ratio of the count rate on the transmission detector with and without the sample is the sample transmission (T_{wide}) due to attenuation from incoherent scattering and absorption.

5.4.2. Rocking curve transmission

Rotating the analyzer through the main beam allows the intensity at q = 0 to be measured. The ratio of this intensity with and without the sample gives the transmission of the sample (T_{rock}) due to attenuation from incoherent scattering, absorption and coherent small angle scattering.

5.5. Multiple scattering estimate

The ratio of these separate transmission measurements can be used to estimate the amount of multiple scattering by

$$T_{\mathrm{SAS}} = \frac{T_{\mathrm{Rock}}}{T_{\mathrm{Wide}}} = e^{-\tau} \tag{11}$$

If $T_{SAS} > 0.9$, the multiple scattering effect can be safely ignored. However, if $T_{SAS} < 0.9$, the multiple scattering becomes a concern.

5.6. Simulation of Scattering

Given enough information about the chemical composition of the sample and expected scattering properties, we can simulate the scattering to help us optimize the experimental setup. The reduction and analysis package provided by NCNR [6, 7] contains tools to help you do this.

The simulation takes input about your sample and simulates the data you would expect to collect on the instrument. This can guide you in deciding many of the factors discussed above such as appropriate sample thickness, counting time, and amount of multiple scattering. Additionally, it can help decide on the density of data points to be collected for USANS or the instrument configurations for SANS.

6. Data reduction

Data reduction consists of correcting the measured scattering from the sample for the sources of background discussed in section 4.2 and rescaling the observed, corrected data to an absolute scale of scattering cross section per unit volume. This is done via equation (5) presented previously and reproduced here for reference:

$$I_{cor}(q)_s = \varepsilon I_{beam} \Delta\Omega_A d_s T \left(\frac{d\sum_s(q)}{d\Omega}\right) \quad (12)$$

The beam intensity εI_{beam} is measured by rotating the analyzer through the direct beam at q = 0 with the empty cell in the beam path. The transmission T is measured by taking the ratio of the count rate observed on the transmission detector with and without the sample in the beam path. The solid angle of scattering accepted by the analyzer $\Delta\Omega_A$ is given by

$$\Delta\Omega_A = \left(\frac{\lambda}{2\pi}\right)^2 (2\Delta q_v)\Delta q_h \ , \quad (13)$$

where $2\Delta q_v$ is the total vertical divergence of the beam convoluted with the angular divergence accepted by the detector and Δq_h is the horizontal divergence accepted for the diffraction by monochromator and analyzer crystals. The instrument accepts scattered neutrons with $\pm\Delta q_v$=0.117Å^{-1}. The horizontal resolution Δq_h is measured from the full width at half maximum (fwhm) of the main beam profile obtained by rotating the analyzer through the direct beam. The fwhm when the crystal is properly aligned is 2.00 *arcsec*, equating to $\Delta q_h = 2.55\times10^{-5}$ Å^{-1} (the BT-5 instrument uses a mean wavelength λ=2.38Å), thus the solid angle over which neutrons are accepted by the analyzer is $\Delta\Omega_A$ = 8.6 x10^{-7} ster.

As you may have noted above, the analyzer has very good resolution in the horizontal direction and very poor resolution in the vertical direction as depicted graphically in figure 8. This is referred to as "slit geometry" as opposed to the "pinhole geometry" of a standard SANS instrument – you may be familiar with this from using a Kratky camera for lab-based small angle x-ray scattering. The large difference between the horizontal and vertical resolutions means that the smearing can be treated as that from an "infinite" slit. The measured cross section, $d\Sigma_s / d\Omega(q)$ obtained from data reduction as described above is related to the true differential macroscopic cross section, $d\Sigma / d\Omega(q)$ by the relation [8]:

$$\frac{d\Sigma_S}{d\Omega(q)} = \frac{1}{\Delta q_v}\int_0^{\Delta q_v} \frac{d\Sigma}{d\Omega}\left(\sqrt{q^2+u^2}\right)du \quad (14)$$

Figure 9 compares the scattering from a 1% volume fraction dispersion of 2 μm silica particles with 5% polydispersity in D_2O using pinhole and slit geometries. Note the damping of the oscillations, the change in slope and reduction in intensity. Desmearing the data directly can be done by an iterative convergence method [9] but the desmeared result is very unstable, being sensitive to noise in the data. The preferred method is to make use of equation (14) to smear a model function and fit the smeared data directly. The latter is the method we will employ in the analysis of our data.

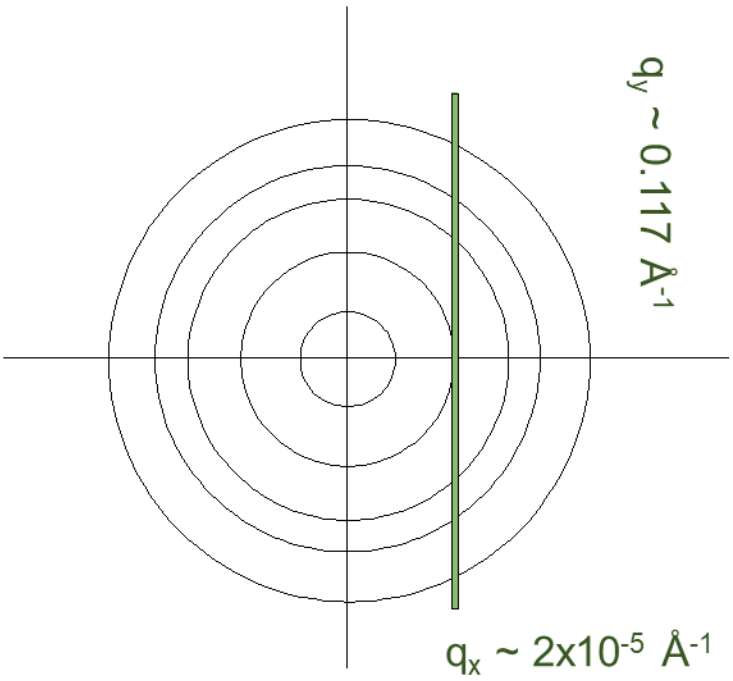

Figure 8: View of scattering with axes q_x and q_y collected by the analyzer on the BT-5 USANS instrument. The circles represent iso-intensity contours from isotropic small angle scattering. The narrow slit represents the scattering region collected by the analyzer.

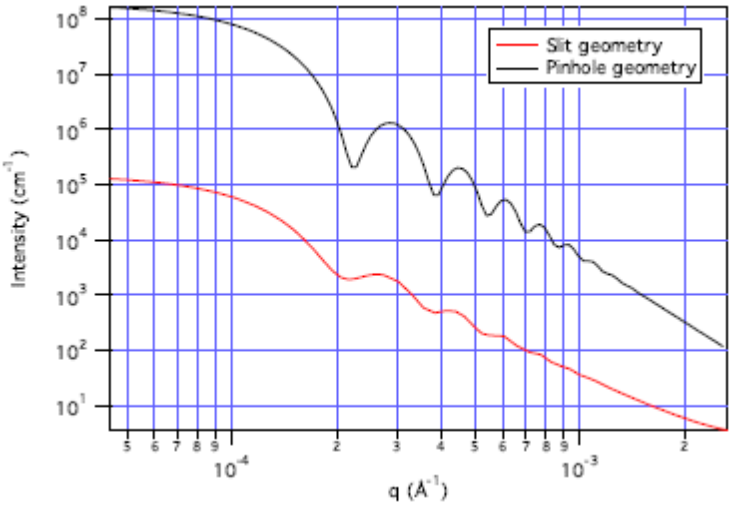

Figure 9: Comparison of the modeled scattering from a 1 % volume fraction dispersion of 2 μm silica particles with 5% polydispersity in D_2O using pinhole and slit geometries.

7. Data Analysis

At the summer school we will use the IGOR USANS/SANS package or SASView to reduce and analyze data collected from samples with different concentrations of microgel to determine:

- The scattering intensity $I_{cor}(q)_s$ for different samples, corrected for background and normalized to absolute intensity, but still slit-smeared by the instrument resolution
- An estimate of the amount of multiple scattering given as T_{SAS} (see Eqn. 11)
- The form factor of the large polystyrene microsphere particle
- The effective inter-particle interaction at different liquid states
- Extract the stickiness parameter τ and the second virial coefficient B_2^* using a model fit with Baxter's model

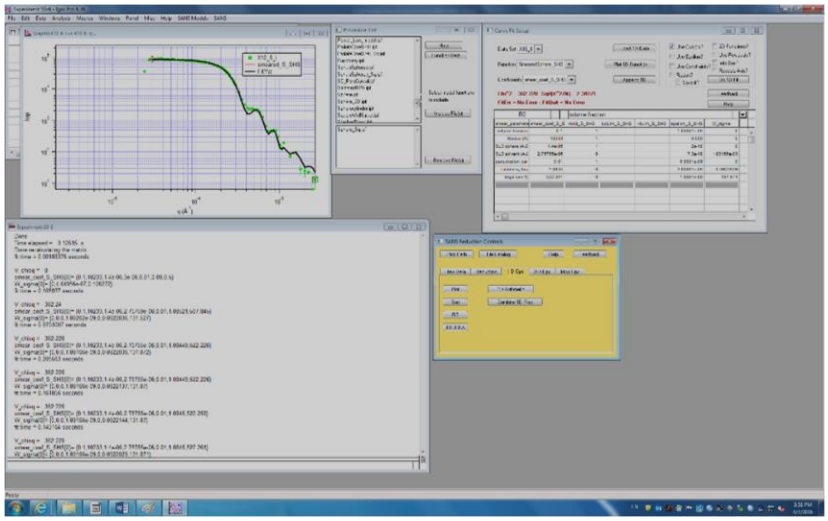

Figure 10: Screenshot of the IGOR program showing various windows relevant to the data fit procedure. The yellow window as well as the "SANS" menu tab are macros downloaded from the NCNR webpage.

8. Summary

Through this experiment you shall learn the following concepts and understand how to apply them to gain useful information from your measurements:

Objectives of the Experiment:

- Get familiar with the USANS technique, how to optimize a sample for USANS and extract useful information from USANS scattering.

- **Determine the form factor of a single Polystyrene microsphere**. This will be measured using a dilute sample without PNIPAM microgel.

- **Determine the** Polystyrene inter-particle interaction for different microgel concentrations. This information is important for the determination of the thermodynamic properties of the systems.

Scattering theory

1) What is the form factor, P(q)
2) What is the inter-particle structure factor, S(q)
3) The scattering contrast between colloidal particle and solvent
4) For a monodisperse system, $I(q) = AP(q)S(q)$
5) The colloidal interaction information can be extracted by fitting I(q)

Instrument information

1) The general principle of USANS
2) Transmission and scattering
3) Multiple scattering
4) Resolution functions
5) Counting statistics

Science from this particular sample system

1) For spherical colloidal systems with short-ranged attractions, the equilibrium phase diagram can be approximated by the sticky hard sphere systems, whose phase diagram can be plotted either in τ-ϕ plane or B_2*-ϕ plane.
2) For the sample condition we investigate in our experiment, we can find the relation between the gelation transition and the gas-liquid transition line.

References

[1] Jean-Pierre Hansen and Ian R. McDonald, "Theory of Simple Liquids";
C. Caccamo, "Integral Equation Theory Description of Phase Equilibria in Classical Fluids", Physics Report 274, 1-105(1996)
[2] J. Luo et al., "Gelation of large hard particles with short-range attraction induced by bridging of small soft microgels ",Soft Matter, 2015, 11, 2494–2503
[3] R. J. Baxter. *J. Chem. Phys.*, 49:2770, 1968.
[4] P. J. Lu, E. Zaccarelli, F. Ciulla, A. B. Scho_eld, F. Sciortino, and D. A. Weitz. *Nature*, 453:499, 2008.
[5] The scattering length is listed at the NCNR website at https://www.ncnr.nist.gov/resources/n-lengths/ . There is also an online tool to help estimate the scattering length density of different tools: https://www.ncnr.nist.gov/resources/activation/
[6] Schelten, J.; Schmatz, W. "Multiple-scattering treatment for small-angle scattering problems" J. Appl. Cryst. 1992, 13, 385-390
[7] http://www.ncnr.nist.gov/programs/sans/data/red anal.html
[8] Roe, R.J. Meth. of X-Ray and Neutron Scattering in Polymer Science, Oxford University, Press, 2000
[9] Lake, J. Acta. Cryst. 1967, 23, 191-194